

Theory of the Casimir interaction for graphene-coated substrates using the polarization tensor and comparison with experiment

G. L. Klimchitskaya,^{1,2} U. Mohideen,³ and V. M. Mostepanenko^{1,2}

¹*Central Astronomical Observatory at Pulkovo of the Russian Academy of Sciences, St.Petersburg, 196140, Russia*

²*Institute of Physics, Nanotechnology and Telecommunications, St.Petersburg State Polytechnical University, St.Petersburg, 195251, Russia*

³*Department of Physics and Astronomy, University of California, Riverside, California 92521, USA*

Abstract

We propose a theory of the thermal Casimir interaction for multilayered test bodies coated with a graphene sheet. The reflection coefficients on such structures are expressed in terms of the components of the polarization tensor and the dielectric permittivities of material layers. The developed theory is applied to calculate the gradient of the Casimir force between an Au-coated sphere and a graphene sheet deposited on a SiO₂ film covering a Si plate, which is the configuration of a recent experiment performed by means of a dynamic atomic force microscope. The theoretical results are found to be in very good agreement with the experimental data. We thus confirm that graphene influences the Casimir interaction and can be used for tailoring the force magnitude in nanostructures.

PACS numbers: 12.20.Ds, 78.67.Wj, 65.80.Ck, 12.20.Fv

I. INTRODUCTION

Graphene is a 2D sheet of carbon atoms which finds diverse applications in nanotechnology and other fields due to its unusual electrical, mechanical and optical properties [1]. As a potential element of nano- and microelectromechanical devices, graphene can be separated by distances of the order of tens or hundreds of nanometers from the other elements. These are the distances at which the van der Waals and Casimir forces caused by the zero-point and thermal fluctuations of the electromagnetic field become dominant [2]. That is why the fluctuation induced *dispersion* forces from graphene have attracted considerable attention in the last few years.

Many papers have been devoted to the calculation of van der Waals and Casimir forces between two graphene sheets [3–11], a graphene sheet and a material plate made of metallic, semiconductor or dielectric materials [4–9, 12–14], a graphene sheet and an atom, a molecule, or other polarizable particle [15–18]. The calculations of the free energies and forces were performed using the Lifshitz theory [19] or its equivalent combined with the reflection coefficients on graphene expressed via some version of the density-density correlation function [5, 6, 8, 9, 18] or the polarization tensor for graphene defined in (2+1)-dimensional space-time [4, 7, 10, 11, 13, 15, 17]. It was found [5, 7, 10, 11, 13, 17, 20] that the thermal Casimir force in graphene systems is qualitatively different from the case of plates made of conventional materials where the classical regime holds at separations exceeding the so-called *thermal length* equal to a few micrometers at room temperature [11, 21]. However for the configuration of two parallel graphene sheets, the classical behavior of the Casimir interaction, characteristic for the case of large separations (high temperatures), holds at separations exceeding a few hundred nanometers [5, 7, 10], i.e., for an order of magnitude shorter separations than for conventional materials.

Measurements of the Casimir force between two freestanding graphene sheets present additional difficulties, as compared to the case of metallic or semiconductor surfaces (see Refs. [22–24] for a review of experiments on measuring the Casimir force). Because of this, in the pioneering experiment [25] the gradient of the Casimir force was measured between an Au-coated sphere and a graphene sheet deposited on a SiO₂ film covering a Si plate. Measurements have been performed by means of a dynamic atomic force microscope (AFM) operated in the frequency-shift technique, i.e., using a method well tested in previous

experiments with metallic test bodies [26–31] and demonstrated its high efficiency. However, the comparison of experiment with theory in Ref. [25] used an approximate additive method where the gradients of the Casimir force between a Si-SiO₂ system and an Au-coated sphere, and between a graphene sheet described by the Dirac model and the same sphere, were computed independently and then added. Such an approximation was applied in the absence of exact reflection coefficients for graphene deposited on a substrate at nonzero temperature (the available reflection coefficients [9, 32, 33] were expressed in terms of the density-density correlation function or, equivalently, the conductivity of graphene whose explicit dependence on the temperature remained unknown). As a result, the theoretical force gradient computed using an assumption of additivity overestimated the measured force gradient. This was explained [25] by the fact that an additive method does not take into account the screening of the SiO₂ surface by the graphene layer. Thus, up to now a complete quantitative theory explaining the measurement data of Ref. [25] has been missing leading to some uncertainty in the demonstrated influence of graphene on the Casimir force.

In this paper, we express the reflection coefficients for a graphene sheet deposited on a multilayered substrate made of conventional materials via the components of the polarization tensor defined at any nonzero temperature and the dielectric permittivities of substrates. The obtained reflection coefficients coincide with those found recently by another method [34]. Then, we substitute the obtained reflection coefficients in the Lifshitz theory and calculate the gradient of the Casimir force in the experimental configuration of Ref. [25] with no additional assumptions or fitting parameters. We demonstrate that the experimental data are in a very good agreement with theory within the limits of experimental errors. Thus, the developed theory confirms the demonstration of the Casimir force from graphene in Ref. [25] and can be used for interpretation of future experiments on measuring the Casimir interaction from graphene deposited on multilayered material substrates.

The paper is organized as follows. In Sec. II we express the reflection coefficients from graphene deposited on a thick material plate (semispace) in terms of the components of the polarization tensor. Section III contains the generalization of these reflection coefficients for graphene deposited on a multilayered substrate and the comparison between the developed theory and the experimental data of Ref. [25]. In Sec. IV the reader will find our conclusions and discussion.

II. REFLECTION COEFFICIENTS FROM GRAPHENE ON A SUBSTRATE IN TERMS OF THE POLARIZATION TENSOR

First, we consider a thin film spaced above a thick plate (semispace) parallel to it in vacuum separated by a gap of thickness d . Let the film be characterized by the amplitude reflection coefficient r_1 and the transmission coefficient t_1 , and the plate be characterized by the amplitude reflection coefficient r_2 (we are interested in the reflection coefficients calculated along the imaginary frequency axis $\omega = i\xi$). Note that the amplitude coefficients correspond to ratios of the reflected (transmitted) complex-valued amplitudes of the electric field to that of the incident field. They are different from the power coefficients which are the fractions of the incident power that is reflected or refracted at the interface. Then, taking into account multiple reflections on the plane of the film and on the upper boundary plane of the plate, one obtains the reflection coefficient R on the system consisting of the film, the gap and the plate (see, for instance, Ref. [35])

$$\begin{aligned} R &= r_1 + t_1 r_2 t_1 e^{-2dq} \sum_{n=0}^{\infty} (r_1 r_2 e^{-2dq})^n \\ &= r_1 + \frac{t_1 r_2 t_1 e^{-2dq}}{1 - r_1 r_2 e^{-2dq}}, \end{aligned} \quad (1)$$

where

$$q = \left(k_{\perp}^2 + \frac{\xi^2}{c^2} \right)^{1/2} \quad (2)$$

and k_{\perp} is the projection of the wave vector on the plane of the film. Note that Eq. (1) is applicable to both the transverse magnetic (TM) and transverse electric (TE) reflection coefficients defined for the two independent polarizations of the electromagnetic field.

Now we apply Eq. (1) to a graphene sheet (g) spaced at a height d above a material semispace (s) characterized by the frequency-dependent dielectric permittivity $\varepsilon_1(i\xi)$. We consider in succession the cases of TM and TE reflection coefficients. Although for the TM polarization of the electromagnetic field there is no general relationship between the amplitude reflection and transmission coefficients [36], for a graphene sheet in vacuum it can be shown that [33]

$$t_{\text{TM}}^{(g)} = 1 - r_{\text{TM}}^{(g)}. \quad (3)$$

Then, by putting $r_1 = r_{\text{TM}}^{(g)}$, $t_1 = t_{\text{TM}}^{(g)}$ and $r_2 = r_{\text{TM}}^{(s)}$ in Eq. (1), and using Eq. (3), one obtains

$$\begin{aligned} R_{\text{TM}}^{(g,s)} &= r_{\text{TM}}^{(g)} + \frac{t_{\text{TM}}^{(g)} r_{\text{TM}}^{(s)} t_{\text{TM}}^{(g)} e^{-2dq}}{1 - r_{\text{TM}}^{(g)} r_{\text{TM}}^{(s)} e^{-2dq}} \\ &= \frac{r_{\text{TM}}^{(g)} + r_{\text{TM}}^{(s)} \left(1 - 2r_{\text{TM}}^{(g)}\right) e^{-2dq}}{1 - r_{\text{TM}}^{(g)} r_{\text{TM}}^{(s)} e^{-2dq}}. \end{aligned} \quad (4)$$

In order to obtain the reflection coefficient from graphene deposited on a thick plate (semispace), we put $d \rightarrow 0$ in Eq. (4) and arrive at

$$R_{\text{TM}}^{(g,s)} = \frac{r_{\text{TM}}^{(g)} + r_{\text{TM}}^{(s)} \left(1 - 2r_{\text{TM}}^{(g)}\right)}{1 - r_{\text{TM}}^{(g)} r_{\text{TM}}^{(s)}}. \quad (5)$$

Note that Eq. (1) was used in Ref. [18] for application to the TM mode of the electromagnetic field, but with an incorrect relationship $t_{\text{TM}}^{(g)} = 1 + r_{\text{TM}}^{(g)}$ instead of Eq. (3).

For a graphene sheet in vacuum the TM reflection coefficient in terms of the polarization tensor takes the form [7]

$$r_{\text{TM}}^{(g)} \equiv r_{\text{TM}}^{(g)}(i\xi, k_{\perp}) = \frac{q\Pi_{00}(i\xi, k_{\perp})}{q\Pi_{00}(i\xi, k_{\perp}) + 2\hbar k_{\perp}^2}, \quad (6)$$

where an exact expression for the 00-component of the polarization tensor Π_{00} in (2+1)-dimensional space-time can be found in Refs. [7, 10, 13, 17] (see Sec. III for the expression used in computations). Note that Π_{00} depends on the temperature as a parameter.

The TM reflection coefficient on the boundary between a vacuum and a semispace is the well known Fresnel coefficient [2, 19]

$$r_{\text{TM}}^{(s)} \equiv r_{\text{TM}}^{(s)}(i\xi, k_{\perp}) = \frac{\varepsilon_1(i\xi)q - k_1}{\varepsilon_1(i\xi)q + k_1}, \quad (7)$$

where

$$k_1 \equiv k_1(i\xi, k_{\perp}) = \left[k_{\perp}^2 + \varepsilon_1(i\xi) \frac{\xi^2}{c^2} \right]^{1/2}. \quad (8)$$

Substituting Eq. (7) in Eq. (5), we arrive at the TM reflection coefficient from the graphene sheet deposited on a material semispace

$$R_{\text{TM}}^{(g,s)}(i\xi, k_{\perp}) = \frac{\varepsilon_1 q + k_1 \left(\frac{q}{\hbar k_{\perp}^2} \Pi_{00} - 1 \right)}{\varepsilon_1 q + k_1 \left(\frac{q}{\hbar k_{\perp}^2} \Pi_{00} + 1 \right)}, \quad (9)$$

where $\Pi_{00} \equiv \Pi_{00}(i\xi, k_{\perp})$ and $\varepsilon_1 \equiv \varepsilon_1(i\xi)$.

For convenience in computations, we express Eq. (9) in terms of the dimensionless variables

$$y = 2aq, \quad \zeta = 2a\xi/c \quad (10)$$

leading to

$$k_1 = \frac{1}{2a} [y^2 + (\varepsilon_1 - 1)\zeta^2]^{1/2}. \quad (11)$$

The reflection coefficient (9) in terms of the new variables takes the form

$$R_{\text{TM}}^{(g,s)}(i\zeta, y) = \frac{\varepsilon_1 y + \sqrt{y^2 + (\varepsilon_1 - 1)\zeta^2} \left(\frac{y}{y^2 - \zeta^2} \tilde{\Pi}_{00} - 1 \right)}{\varepsilon_1 y + \sqrt{y^2 + (\varepsilon_1 - 1)\zeta^2} \left(\frac{y}{y^2 - \zeta^2} \tilde{\Pi}_{00} + 1 \right)}, \quad (12)$$

where

$$\tilde{\Pi}_{00} \equiv \tilde{\Pi}_{00}(i\zeta, y) = \frac{2a}{\hbar} \Pi_{00} \quad (13)$$

is the dimensionless polarization tensor [10, 13, 17].

We now proceed with the case of the TE reflection coefficient for a graphene sheet at a height d in vacuum above a semispace. There is a general relationship between the amplitude reflection and transmission coefficients in the case of TE polarization of the electromagnetic field [36]

$$t_{\text{TE}}^{(g)} = 1 + r_{\text{TE}}^{(g)}. \quad (14)$$

Substituting this in Eq. (1) and putting $r_1 = r_{\text{TE}}^{(g)}$, $t_1 = t_{\text{TE}}^{(g)}$ and $r_2 = r_{\text{TE}}^{(s)}$, we obtain

$$\begin{aligned} R_{\text{TE}}^{(g,s)} &= r_{\text{TE}}^{(g)} + \frac{t_{\text{TE}}^{(g)} r_{\text{TE}}^{(s)} t_{\text{TE}}^{(g)} e^{-2dq}}{1 - r_{\text{TE}}^{(g)} r_{\text{TE}}^{(s)} e^{-2dq}} \\ &= \frac{r_{\text{TE}}^{(g)} + r_{\text{TE}}^{(s)} \left(1 + 2r_{\text{TE}}^{(g)} \right) e^{-2dq}}{1 - r_{\text{TE}}^{(g)} r_{\text{TE}}^{(s)} e^{-2dq}}. \end{aligned} \quad (15)$$

In the limiting case $d \rightarrow 0$ one obtains from Eq. (15) the TE reflection coefficient for a graphene deposited on a semispace

$$R_{\text{TE}}^{(g,s)} = \frac{r_{\text{TE}}^{(g)} + r_{\text{TE}}^{(s)} \left(1 + 2r_{\text{TE}}^{(g)} \right)}{1 - r_{\text{TE}}^{(g)} r_{\text{TE}}^{(s)}}. \quad (16)$$

The TE reflection coefficient for a graphene sheet in vacuum is given by [7]

$$r_{\text{TE}}^{(g)} \equiv r_{\text{TE}}^{(g)}(i\xi, k_{\perp}) = -\frac{k_{\perp}^2 \Pi_{\text{tr}}(i\xi, k_{\perp}) - q^2 \Pi_{00}(i\xi, k_{\perp})}{k_{\perp}^2 \Pi_{\text{tr}}(i\xi, k_{\perp}) - q^2 \Pi_{00}(i\xi, k_{\perp}) + 2\hbar k_{\perp}^2 q}, \quad (17)$$

where the exact expression for Π_{tr} can be found in Refs. [7, 10, 13, 17] (see also Sec. III).

The Fresnel TE reflection coefficient from a semispace to a vacuum is given by [2, 19]

$$r_{\text{TE}}^{(s)} \equiv r_{\text{TE}}^{(s)}(i\xi, k_{\perp}) = \frac{q - k_1}{q + k_1}. \quad (18)$$

Substituting Eqs. (17) and (18) in Eq. (16), one obtains the TE reflection coefficient from the graphene sheet deposited on a semispace

$$R_{\text{TE}}^{(g,s)}(i\xi, k_{\perp}) = \frac{q - k_1 - \frac{1}{\hbar k_{\perp}^2} (k_{\perp}^2 \Pi_{\text{tr}} - q^2 \Pi_{00})}{q + k_1 + \frac{1}{\hbar k_{\perp}^2} (k_{\perp}^2 \Pi_{\text{tr}} - q^2 \Pi_{00})}, \quad (19)$$

where $\Pi_{\text{tr}} \equiv \Pi_{\text{tr}}(i\xi, k_{\perp})$. If we take into account the connections between the polarization tensor and the temperature-dependent density-density correlation functions and nonlocal dielectric permittivities found in Ref. [34], it can be seen that the reflection coefficients (9) and (19) coincide with the respective coefficients derived in Refs. [9, 32, 33] from the exact electrodynamic boundary conditions.

In terms of dimensionless variables (10) the reflection coefficient (19) takes the form

$$R_{\text{TE}}^{(g,s)}(i\zeta, y) = \frac{y - \sqrt{y^2 + (\varepsilon_1 - 1)\zeta^2} - \left(\tilde{\Pi}_{\text{tr}} - \frac{y^2}{y^2 - \zeta^2} \tilde{\Pi}_{00} \right)}{y + \sqrt{y^2 + (\varepsilon_1 - 1)\zeta^2} + \left(\tilde{\Pi}_{\text{tr}} - \frac{y^2}{y^2 - \zeta^2} \tilde{\Pi}_{00} \right)}, \quad (20)$$

where

$$\tilde{\Pi}_{\text{tr}} \equiv \tilde{\Pi}_{\text{tr}}(i\zeta, y) = \frac{2a}{\hbar} \Pi_{\text{tr}}. \quad (21)$$

The representation (20) is convenient for use in numerical computations.

III. COMPARISON BETWEEN EXPERIMENT AND THEORY

In the experiment of Ref. [25] the gradient of the Casimir force was measured between an Au-coated hollow glass sphere of radius $R = 54.1 \mu\text{m}$ and a large area graphene sheet deposited on a $D = 300 \text{ nm}$ thick SiO_2 film covering a B-doped Si plate of $500 \mu\text{m}$ thickness. The thickness of the Au coating on the sphere was measured to be 280 nm . With respect to the Casimir force, the sphere can be considered as completely gold and the Si plate as an infinitely thick semispace [2]. However, the exact thickness of the SiO_2 film should be taken into account in computations of the theoretical Casimir force.

In the dynamic measurement scheme by means of the AFM the sphere was attached to a cantilever oscillating with the natural resonant frequency ω_0 . Under the influence of the external force, electric and Casimir, the resonant frequency was modified. The change in

the frequency $\Delta\omega = \omega_r - \omega_0$, where ω_r is the resonance frequency in the presence of external force, was measured by means of a phase-locked loop and recorded as a function of separation a between the sphere and graphene surfaces. This frequency change is proportional to the gradient of the external force.

Measurements were performed in high vacuum down to 10^{-9} Torr with two graphene samples in two different ways. In the first case, after the electrostatic calibration (i.e., determination of the calibration constant, residual potential difference, and the separation at the closest approach between the test bodies by applying different voltages), the gradient of the Casimir force was subtracted from the total measured force gradient resulting in the gradient of the Casimir force. In the second case, only the compensating voltage equal to the residual potential difference was applied to graphene, and the gradient of the Casimir force was an immediately measured quantity.

Altogether 84 force-distance relations have been measured (20 with different applied voltages and 22 with applied compensating voltage for each of the two graphene samples). All the results were found to be in a very good mutual agreement in the limits of the experimental errors [25]. Below we perform the theory-experiment comparison for the two sets of mean measured gradients of the Casimir force obtained for the two graphene samples with applied compensating voltages. In this case the total error of the measured gradients of the Casimir force is slightly smaller than for the other two sets with subtracted electrostatic forces because the latter are calculated with some errors which should be added to the total experimental error common to both ways of measurement.

In Figs. 1 and 2 the mean gradients of the Casimir force, measured [25] for the first and second graphene samples, are indicated as crosses. The averaging was performed over 22 force-distance relations obtained for each of the two samples. The horizontal arms of the crosses indicate twice the error $\Delta a = 0.4$ nm in measurements of absolute separations between the surfaces. The vertical arms are twice the error $\Delta F' = 0.64$ $\mu\text{N}/\text{m}$ in measurements of the gradient of the Casimir force. All errors are indicated at the 67% confidence level. Measurements were performed over the separation region from 224 to 500 nm.

The gradient of the Casimir force between an Au sphere and graphene sheet deposited on a SiO_2 film covering a Si plate (semispace) was calculated using the Lifshitz formula in the proximity force approximation [2]. For convenience in computations, we use the

dimensionless variables (10) and obtain

$$F'(a) = \frac{k_B T R}{4a^3} \sum_{l=0}^{\infty} \int_{\zeta_l}^{\infty} y^2 dy \left[\frac{r_{\text{TM}}^{(\text{Au})}(i\zeta_l, y) R_{\text{TM}}^{(g,f,s)}(i\zeta_l, y)}{e^y - r_{\text{TM}}^{(\text{Au})}(i\zeta_l, y) R_{\text{TM}}^{(g,f,s)}(i\zeta_l, y)} + \frac{r_{\text{TE}}^{(\text{Au})}(i\zeta_l, y) R_{\text{TE}}^{(g,f,s)}(i\zeta_l, y)}{e^y - r_{\text{TE}}^{(\text{Au})}(i\zeta_l, y) R_{\text{TE}}^{(g,f,s)}(i\zeta_l, y)} \right], \quad (22)$$

where k_B is the Boltzmann constant, $T = 300$ K is the temperature at the laboratory, and the dimensionless quantities $\zeta_l = 2a\xi_l/c$ are expressed via the Matsubara frequencies $\xi_l = 2\pi k_B T l / \hbar$ with $l = 0, 1, 2, \dots$. Note that under the condition $a \ll R$, which is satisfied in our case with a wide safety margin, the corrections to PFA in sphere-plate geometry are negligibly small [37–40]. Now we specify the reflection coefficients $r_{\text{TM,TE}}^{(\text{Au})}$ and $R_{\text{TM,TE}}^{(g,f,s)}$ entering Eq. (22).

The first of them is the standard amplitude Fresnel coefficient on the Au semispace given by Eqs. (7) and (18). In terms of dimensionless variables, for the TM and TE polarizations, it is given by

$$r_{\text{TM}}^{(\text{Au})}(i\zeta_l, y) = \frac{\varepsilon_l^{(\text{Au})} y - \sqrt{y^2 + (\varepsilon_l^{(\text{Au})} - 1)\zeta_l^2}}{\varepsilon_l^{(\text{Au})} y + \sqrt{y^2 + (\varepsilon_l^{(\text{Au})} - 1)\zeta_l^2}},$$

$$r_{\text{TE}}^{(\text{Au})}(i\zeta_l, y) = \frac{y - \sqrt{y^2 + (\varepsilon_l^{(\text{Au})} - 1)\zeta_l^2}}{y + \sqrt{y^2 + (\varepsilon_l^{(\text{Au})} - 1)\zeta_l^2}}, \quad (23)$$

where $\varepsilon_l^{(\text{Au})} \equiv \varepsilon^{(\text{Au})}(ic\zeta_l/2a)$. The latter quantity is found (see reviews [2, 22] and references therein) by means of the Kramers-Kronig relation from the optical data for $\text{Im}\varepsilon^{(\text{Au})}$ given over a wide frequency range in Ref. [41] and extrapolated to zero frequency. It is well known [2, 22] that there are two approaches to this extrapolation using the Drude and the plasma models leading to different results for the thermal Casimir force between two metallic surfaces. For a metallic surface interacting with graphene the differences arising from the use of two approaches are, however, negligibly small [13, 25] and are included here into the magnitude of the theoretical error.

The reflection coefficients from a graphene sheet deposited on a SiO_2 film covering a Si plate, $R_{\text{TM,TE}}^{(g,f,s)}$, can be written using the formalism, developed in Sec. II and the standard formulas of the Lifshitz theory describing the reflection coefficients from planar layered

structures [2, 42, 43]

$$R_{\text{TM,TE}}^{(g,f,s)}(i\zeta_l, y) = \frac{R_{\text{TM,TE}}^{(g,s)}(i\zeta_l, y) + r_{\text{TM,TE}}^{(f,s)}(i\zeta_l, y)e^{-2Dk_1}}{1 + R_{\text{TM,TE}}^{(g,s)}(i\zeta_l, y)r_{\text{TM,TE}}^{(f,s)}(i\zeta_l, y)e^{-2Dk_1}}, \quad (24)$$

where k_1 is defined in Eq. (11). The reflection coefficients $R_{\text{TM,TE}}^{(g,s)}$ are given in Eqs. (12) and (20), respectively. They describe the reflection from a graphene sheet deposited on a SiO₂ semispace, and, thus, $\varepsilon_1 = \varepsilon^{(\text{SiO}_2)}(ic\zeta_l/2a) \equiv \varepsilon_{1l}$. The reflection coefficients $r_{\text{TM,TE}}^{(f,s)}$ describe the reflection on the boundary plane between the two semispaces made of SiO₂ and Si. These are the standard, Fresnel, reflection coefficients. In terms of dimensionless variables they are given by

$$\begin{aligned} r_{\text{TM}}^{(f,s)}(i\zeta_l, y) &= \frac{\varepsilon_{2l}k_1 - \varepsilon_{1l}k_2}{\varepsilon_{2l}k_1 + \varepsilon_{1l}k_2} \\ r_{\text{TE}}^{(f,s)}(i\zeta_l, y) &= \frac{k_1 - k_2}{k_1 + k_2}, \end{aligned} \quad (25)$$

where $\varepsilon_{2l} \equiv \varepsilon^{(\text{Si})}(ic\zeta_l/2a)$ and, similar to Eq. (11),

$$k_2 = \frac{1}{2a} [y^2 + (\varepsilon_{2l} - 1)\zeta_l^2]^{1/2}. \quad (26)$$

Now we discuss explicit expressions for all the quantities entering Eq. (24). According to Eqs. (12) and (20), the coefficient $R_{\text{TM,TE}}^{(g,s)}$ depends on the components of the polarization tensor. As was shown in Refs. [7, 10, 13, 17], an explicit dependence of the polarization tensor on T influences the computational results only through the contribution from the zero Matsubara frequency $\zeta_0 = 0$, whereas all contributions with $l \geq 1$ can be calculated with the polarization tensor defined at $T = 0$. Because of this, in computations below we use the following temperature-dependent expressions at $\zeta_0 = 0$ entering Eqs. (12) and (20) [7, 13]

$$\begin{aligned} \tilde{\Pi}_{00}(0, y) &= \frac{8\alpha}{\tilde{v}_F^2} \left[\frac{\tau}{\pi} \int_0^1 dx \ln \left(2 \cosh \frac{\pi\theta}{\tau} \right) \right. \\ &\quad \left. - \tilde{\Delta}^2 \int_0^1 \frac{dx}{\theta} \tanh \frac{\pi\theta}{\tau} \right], \\ \tilde{\Pi}_{\text{tr}}(0, y) - \tilde{\Pi}_{00}(0, y) &= 8\alpha\tilde{v}_F^2 y^2 \int_0^1 dx \frac{x(1-x)}{\theta} \tanh \frac{\pi\theta}{\tau}. \end{aligned} \quad (27)$$

Here, $\alpha = e^2/(\hbar c)$ is the fine-structure constant, $v_F \approx 9 \times 10^5$ m/s is the Fermi velocity in graphene [44, 45], $\tilde{v}_F \equiv v_F/c$, the temperature parameter is $\tau = 4\pi a k_B T/(\hbar c)$, and the

following notation is introduced

$$\theta \equiv \theta(x, y) = \left[\tilde{\Delta}^2 + x(1-x)\tilde{v}_F^2 y^2 \right]^{1/2}, \quad (28)$$

where Δ is gap parameter of graphene and $\tilde{\Delta} \equiv 2a\Delta/(\hbar c)$. The gap parameter takes into account that the Dirac-type excitations in graphene become massive under the influence of electron-electron interaction, substrates, and defects of the structure [46–50]. The exact value of Δ is unknown but its maximum value is estimated as 0.1 eV [4].

At all nonzero Matsubara frequencies one can use in Eqs. (12) and (20) the following expressions found [4, 7, 13] at $T = 0$:

$$\begin{aligned} \tilde{\Pi}_{00}(i\zeta_l, y) &= \alpha \frac{y^2 - \zeta_l^2}{f^2(\zeta_l, y)} \Phi(\zeta_l, y) \\ \tilde{\Pi}_{\text{tr}}(i\zeta_l, y) - \frac{y^2}{y^2 - \zeta_l^2} \tilde{\Pi}_{00}(i\zeta_l, y) &= \alpha \Phi(\zeta_l, y), \end{aligned} \quad (29)$$

where the two notations are introduced

$$\begin{aligned} f(\zeta_l, y) &= [\tilde{v}_F^2 y^2 + (1 - \tilde{v}_F^2)\zeta_l^2]^{1/2}, \\ \Phi(\zeta_l, y) &= 4\tilde{\Delta} + 2f(\zeta_l, y) \left[1 - \frac{4\tilde{\Delta}^2}{f^2(\zeta_l, y)} \right] \arctan \frac{f(\zeta_l, y)}{2\tilde{\Delta}}. \end{aligned} \quad (30)$$

Two more quantities, which are needed to calculate the reflection coefficients (25), are the dielectric permittivities of Si and SiO₂ at the imaginary Matsubara frequencies. The Si plate used in Ref. [25] had a resistivity between 0.001 and 0.005 Ω cm, which corresponds [51] to a charge carrier density $n \approx (1.6 \div 7.8) \times 10^{19} \text{ cm}^{-3}$. For B-doped Si the dielectric-to-metal transition occurs [52] at $n_c \approx 3.95 \times 10^{18} \text{ cm}^{-3}$. Thus, the Si used was of metal-type with the plasma frequency ω_p between $5 \times 10^{14} \text{ rad/s}$ and $11 \times 10^{14} \text{ rad/s}$ [53] and $\gamma \approx 1.1 \times 10^{14} \text{ rad/s}$ for the relaxation parameter [25]. In our computations we used $\varepsilon_{2l} = \varepsilon^{(\text{Si})}(i\xi_l)$ obtained [54] by means of the Kramers-Kronig relation from the optical data [55] extrapolated to zero frequency either by the Drude or by the plasma model. Similar to the case of Au interacting with graphene, here different types of extrapolation lead to only a minor differences in the resulting force gradients which are included in the theoretical error. As to the dielectric permittivity $\varepsilon_{1l} = \varepsilon^{(\text{SiO}_2)}(i\xi_l)$, a sufficiently accurate expression for it presented in Ref. [56] was used in computations.

Finally, the gradients of the Casimir force in the experimental configuration of Ref. [25] were computed by Eq. (22) with the reflection coefficients presented in Eqs. (23) and (24).

The obtained force gradients were corrected for the presence of surface roughness on both surfaces. For this purpose the rms roughness was measured by means of AFM and found to be equal to 1.6 and 1.5 nm on the sphere and graphene, respectively. It was taken into account using the multiplicative approach [2, 22] which is sufficiently precise for so small roughness at relatively large separations above 200 nm. It was shown that maximum contribution of roughness to the force gradient achieved at the shortest separation of $a = 224$ nm is equal to only 0.1% of the calculated results.

The computed gradients of the Casimir force are shown as gray bands in Figs. 1(a-d) and 2(a-d) in comparison with the experimental data obtained for the first and second graphene samples, respectively. The widths of the bands are determined by the uncertainty in the value of ω_p for a Si plate within the interval indicated above, differences between the predictions of the Drude and plasma model extrapolations of the optical data for Au and Si, and by the uncertainty of the mass gap parameter of graphene within the interval from 0 to 0.1 eV. As can be seen in Figs. 1 and 2, our theory describing the reflection coefficients from graphene deposited on a substrate in terms of the polarization tensor is in a very good agreement with the measurement data.

To make the advantages of the suggested theory more transparent, we again present in Fig. 3 the experimental data for F' obtained with the first graphene sample in comparison with the two gray theoretical bands. The lower band shows the gradient of the Casimir force between an Au-coated sphere and a substrate consisting of a SiO₂ film covering a Si plate with no graphene coating calculated using the standard Lifshitz theory (measurement of this force gradient presents difficulties due to electric charges localized on the dielectric surface). The upper band shows the force gradient between an Au-coated sphere and graphene deposited on this substrate obtained using an additive approach (i.e., computed by adding the force gradient from Au-graphene interaction to the lower band). As can be seen from the figure, the lower band underestimates whereas the upper band overestimates the measured force gradients. The latter was explained in Ref. [25] by the fact that the additive approach does not take into account the screening of the SiO₂ film by the graphene sheet. The theory developed here takes the effects of nonadditivity into account and brings theoretical predictions in agreement with the measurement data.

IV. CONCLUSIONS AND DISCUSSION

In the foregoing, we have developed a theory of the Casimir interaction for a graphene deposited on multilayered substrate made of ordinary materials. The reflection coefficients on substrates coated with graphene were expressed via components of the polarization tensor of graphene in (2+1)-dimensional space-time and dielectric permittivities of substrate materials in the imaginary Matsubara frequencies. The suggested theory allows calculation of the Casimir interaction between two graphene-coated multilayered structures and between the test body made of an ordinary material and the graphene-coated multilayered substrate at any temperature. It allows generalization for the case of doped graphene sheets.

The developed theory was applied to the configuration of the experiment [25] on measuring the gradient of the Casimir force between an Au-coated sphere and a graphene sheet deposited on a SiO₂ film covering a Si plate. Previously the measurement data of this experiment was compared with only an approximate additive theory and agreement with the computational results was not achieved. We have performed computations of the gradient of the Casimir force using the reflection coefficients on a multilayered substrate coated with graphene which are expressed via the polarization tensor. Good agreement between the new theory and the measurement data was demonstrated with no fitting parameters in the limits of the experimental errors and uncertainties.

The achieved agreement between the experimental data and the complete theory applicable to a graphene deposited on substrates allows to conclude with certainty that the experiment of Ref. [25] demonstrates influence of graphene sheet on the Casimir interaction. This conclusion opens prospective opportunities for tailoring the Casimir force in nanostructures by using graphene.

Acknowledgments

This work was supported by the DOE Grant No. DEF010204ER46131 (U.M.). The authors are grateful to Bo E. Sernelius for stimulating discussions.

- [1] M. I. Katsnelson, *Graphene: Carbon in Two Dimensions* (Cambridge University Press, Cambridge, 2012).
- [2] M. Bordag, G. L. Klimchitskaya, U. Mohideen, and V. M. Mostepanenko, *Advances in the Casimir Effect* (Oxford University Press, Oxford, 2009).
- [3] J. F. Dobson, A. White, and A. Rubio, Phys. Rev. Lett. **96**, 073201 (2006).
- [4] M. Bordag, I. V. Fialkovsky, D. M. Gitman, and D. V. Vassilevich, Phys. Rev. B **80**, 245406 (2009).
- [5] G. Gómes-Santos, Phys. Rev. B **80**, 245424 (2009).
- [6] D. Drosdoff and L. M. Woods, Phys. Rev. B **82**, 155459 (2010).
- [7] I. V. Fialkovsky, V. N. Marachevsky, and D. V. Vassilevich, Phys. Rev. B **84**, 035446 (2011).
- [8] Bo E. Sernelius, Europhys. Lett. **95**, 57003 (2011).
- [9] Bo E. Sernelius, Phys. Rev. B **85**, 195427 (2012).
- [10] G. L. Klimchitskaya and V. M. Mostepanenko, Phys. Rev. B **87**, 075439 (2013).
- [11] G. L. Klimchitskaya and V. M. Mostepanenko, Phys. Rev. B **89**, 035407 (2014).
- [12] D. Drosdoff and L. M. Woods, Phys. Rev. A **84**, 062501 (2011).
- [13] M. Bordag, G. L. Klimchitskaya, and V. M. Mostepanenko, Phys. Rev. B **86**, 165429 (2012).
- [14] A. D. Phan, L. M. Woods, D. Drosdoff, I. V. Bondarev, and N. A. Viet, Appl. Phys. Lett. **101**, 113118 (2012).
- [15] Yu. V. Churkin, A. B. Fedortsov, G. L. Klimchitskaya, and V. A. Yurova, Phys. Rev. B **82**, 165433 (2010).
- [16] T. E. Judd, R. G. Scott, A. M. Martin, B. Kaczmarek, and T. M. Fromhold, New. J. Phys. **13**, 083020 (2011).
- [17] M. Chaichian, G. L. Klimchitskaya, V. M. Mostepanenko, and A. Tureanu, Phys. Rev. A **86**, 012515 (2012).
- [18] S. Ribeiro and S. Scheel, Phys. Rev. A **88**, 042519 (2013).

- [19] E. M. Lifshitz and L. P. Pitaevskii, *Statistical Physics*, Pt.II (Pergamon Press, Oxford, 1980).
- [20] V. Svetovoy, Z. Moktadir, M. Elvenspoek, and H. Mizuta, *Europhys. Lett.* **96**, 14006 (2011).
- [21] J. Feinberg, A. Mann, and M. Revzen, *Ann. Phys. (NY)* **288**, 103 (2001).
- [22] G. L. Klimchitskaya, U. Mohideen, and V. M. Mostepanenko, *Rev. Mod. Phys.* **81**, 1827 (2009).
- [23] A. W. Rodriguez, F. Capasso, and S. G. Johnson, *Nature Photon.* **5**, 211 (2011).
- [24] G. L. Klimchitskaya, U. Mohideen, and V. M. Mostepanenko, *Int. J. Mod. Phys. B* **25**, 171 (2011).
- [25] A. A. Banishev, H. Wen, J. Xu, R. K. Kawakami, G. L. Klimchitskaya, V. M. Mostepanenko, and U. Mohideen, *Phys. Rev. B* **87**, 205433 (2013).
- [26] C.-C. Chang, A. A. Banishev, R. Castillo-Garza, G. L. Klimchitskaya, V. M. Mostepanenko, and U. Mohideen, *Phys. Rev. B* **85**, 165443 (2012).
- [27] A. A. Banishev, C.-C. Chang, R. Castillo-Garza, G. L. Klimchitskaya, V. M. Mostepanenko, and U. Mohideen, *Int. J. Mod. Phys. A* **27**, 1260001 (2012).
- [28] A. A. Banishev, C.-C. Chang, G. L. Klimchitskaya, V. M. Mostepanenko, and U. Mohideen, *Phys. Rev. B* **85**, 195422 (2012).
- [29] A. A. Banishev, G. L. Klimchitskaya, V. M. Mostepanenko, and U. Mohideen, *Phys. Rev. Lett.* **110**, 137401 (2013).
- [30] A. A. Banishev, G. L. Klimchitskaya, V. M. Mostepanenko, and U. Mohideen, *Phys. Rev. B* **88**, 155410 (2013).
- [31] R. Castillo-Garza, J. Xu, G. L. Klimchitskaya, V. M. Mostepanenko, and U. Mohideen, *Phys. Rev. B* **88**, 075402 (2013).
- [32] L. A. Falkovsky and S. S. Pershoguba, *Phys. Rev. B* **76**, 153410 (2007).
- [33] T. Stauber, N. M. R. Peres, and A. K. Geim, *Phys. Rev. B* **78**, 085432 (2008).
- [34] G. L. Klimchitskaya, V. M. Mostepanenko, and Bo E. Sernelius, *Phys. Rev. B* **89**, 125407 (2014).
- [35] W. C. Chew, *Waves and Fields in Inhomogeneous Media* (Wiley-IEEE Press, New York, 1999).
- [36] E. Hecht, *Optics* (Addison-Wesley, Reading, 2002).
- [37] C. D. Fosco, F. C. Lombardo, and F. D. Mazzitelli, *Phys. Rev. D* **84**, 105031 (2011).
- [38] G. Bimonte, T. Emig, R. L. Jaffe, and M. Kardar, *Europhys. Lett.* **97**, 50001 (2012).
- [39] G. Bimonte, T. Emig, and M. Kardar, *Appl. Phys. Lett.* **100**, 074110 (2012).

- [40] L. P. Teo, Phys. Rev. D **88**, 045019 (2013).
- [41] *Handbook of Optical Constants of Solids*, ed. E. D. Palik (Academic, New York, 1985).
- [42] M. S. Tomaš, Phys. Rev. A **66**, 052103 (2002).
- [43] G. L. Klimchitskaya, U. Mohideen, and V. M. Mostepanenko, J. Phys.: Condens. Matter **24**, 424202 (2012).
- [44] B. Wunsch, T. Stauber, F. Sols, and F. Guinea, New J. Phys. **8**, 318 (2006).
- [45] N. M. R. Peres, F. Guinea, and A. H. Castro Neto, Phys. Rev. B **73**, 125411 (2006).
- [46] A. H. Castro Neto, F. Guinea, N. M. R. Peres, K. S. Novoselov, and A. K. Geim, Rev. Mod. Phys. **81**, 109 (2009).
- [47] S. A. Jafari, J. Phys.: Condens. Matter **24**, 205802 (2012).
- [48] P. K. Pyatkovskiy, J. Phys.: Condens. Matter **21**, 025506 (2009).
- [49] V. P. Gusynin, S. G. Sharapov, and J. P. Carbotte, New J. Phys. **11**, 095013 (2009).
- [50] V. P. Gusynin and S. G. Sharapov, Phys. Rev. B **73**, 245411 (2006).
- [51] *Quick Reference Manual for Silicon Integrated Circuit Technology*, eds. W. E. Beadle, J. C. C. Tsai, and R. D. Plummer (Wiley, New York, 1985).
- [52] P. Dai, Y. Zhang, and M. P. Sarachik, Phys. Rev. Lett. **66**, 1914 (1991).
- [53] *Semiconductors: Physics of Group IV Elements and III-V Compounds*, ed. K.-H. Hellwege (Springer, Berlin, 1982).
- [54] F. Chen, U. Mohideen, G. L. Klimchitskaya, and V. M. Mostepanenko, Phys. Rev. A **72**, 020101(R) (2005); **74**, 022103 (2006).
- [55] *Handbook of Optical Constants of Solids*, vol II, ed. E. D. Palik (Academic, New York, 1991).
- [56] L. Bergström, Adv. Colloid Interface Sci. **70**, 125 (1997).

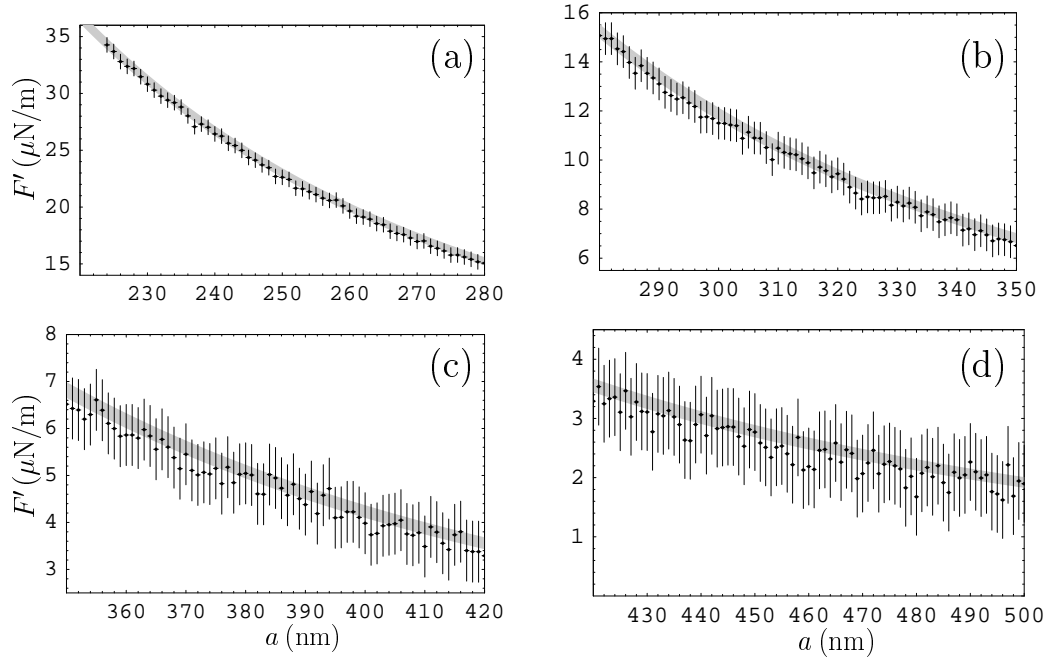


FIG. 1: The experimental data for the gradient of the Casimir force between an Au-coated sphere and graphene deposited on a SiO₂ film covering a Si plate (the first sample) are shown as crosses plotted at a 67% confidence level over different separation regions. The gray bands present the theoretical force gradients computed using the exact reflection coefficients for graphene on a multilayered substrate derived here in terms of the polarization tensor.

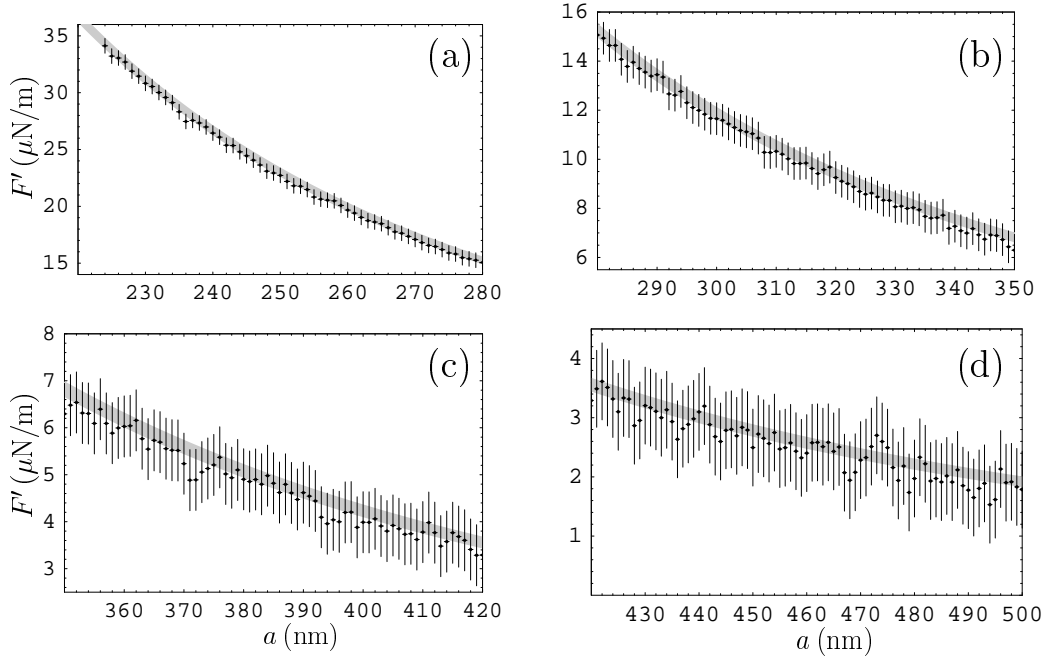


FIG. 2: The experimental data for the gradient of the Casimir force between an Au-coated sphere and graphene deposited on a SiO_2 film covering a Si plate (the second sample) are shown as crosses plotted at a 67% confidence level over different separation regions. The gray bands present the theoretical force gradients computed using the exact reflection coefficients for graphene on a multilayered substrate derived here in terms of the polarization tensor.

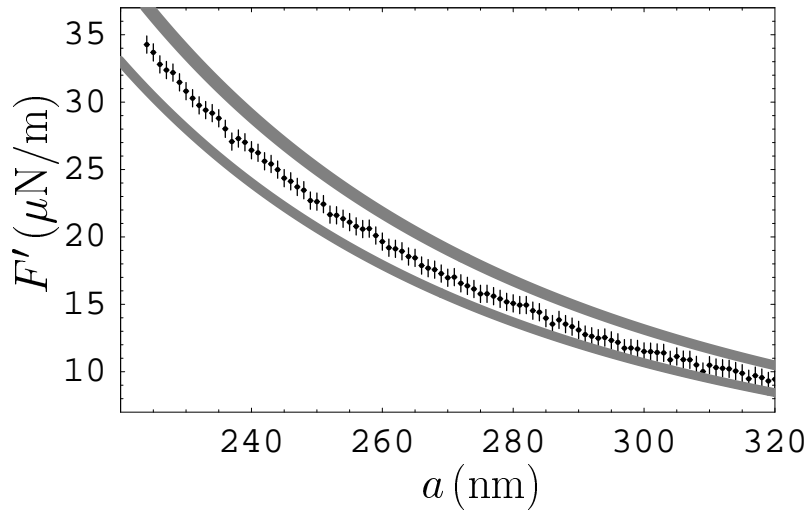


FIG. 3: The experimental data for the gradient of the Casimir force between an Au-coated sphere and graphene deposited on a SiO_2 film covering a Si plate (the first sample) are shown as crosses plotted at a 67% confidence level over the separation region below 320 nm. The gray bands present the theoretical force gradients between an Au-coated sphere and a substrate consisting of a SiO_2 film covering a Si plate computed using the standard Lifshitz theory (the lower band) and between an Au-coated sphere and graphene deposited on this substrate using the additive approach (the upper band).